Characterization of Starburst Dendrimers by the EPR Technique. 1. Copper Complexes in Water Solution

M. Francesca Ottaviani,*,† Stefan Bossmann,‡,§ Nicholas J. Turro,‡ and Donald A. Tomalia∥

Contribution from the Department of Chemistry, University of Florence, 50121 Firenze, Italy, Michigan Molecular Institute, Midland, Michigan 48640, and Department of Chemistry, Columbia University, New York, New York 10027

Received August 4, 1993®

Abstract: The structure of Cu(II) complexes formed with anionic starburst dendrimers (*n*.5 G-SBD) in aqueous solution has been investigated by the electron paramagnetic resonance (EPR) technique. The line shapes of the EPR spectra of the complexes at room temperature show a distinction between earlier ($n < 3$) and later ($n \geq 3$) generations and are consistent with a change of the dendrimer shape, which supports the results of molecular simulation of the dendrimer morphology as a function of generation. The earlier generations appear to possess a more open structure, which leads to a greater mobility of the copper complexes. Three different complexes of copper with groups composing the dendrimer structure are identified by analyzing the spectra as a function of the dendrimer size (generation), the pH, and the temperature. The magnetic parameters, evaluated at low temperature with the aid of spectral computation, indicate that the copper ions form monomeric carboxylate complexes at low pH (signal C). With an increase of pH, the ions interact with nitrogen centers in the internal porous structure of the dendrimers. The complex formed at intermediate pH is identified as a Cu(II)–N_2O_2 complex (signal A). Such a complex, which involves both the carboxylic groups at the dendrimer interface and the internal nitrogen centers, is preferentially formed by low-generation dendrimers. This result is consistent with the morphology of the dendrimer structure. The higher generation dendrimers present a wide number of internal sites in which the tightly packed structure appears to facilitate the interaction with more than two nitrogens. This Cu(II)–N_3O or Cu(II)–N_4 complex gives a third signal (termed signal B), which increases its intensity at the expense of signal A, both with the increase of generation and with the increase of pH. However, the interaction with nitrogen centers in both cases is not strong enough to give superhyperfine structure in the EPR spectra. For freshly prepared samples, formation of the complex with the larger nitrogen coordination corresponds to enhancement in the EPR room temperature spectra of a signal of a nitrogen-centered radical species, which is also observed in the spectra of pure dendrimers. The spectral features of this radical are identified, by spectral computation, as resulting from an unpaired electron which couples with one nitrogen and four protons from two slightly nonequivalent CH_2 groups. Aging of the samples leads to an increase in intensity of signal B, simultaneously with the disappearance of the radical signal. This allows the identification of one of the coordinating sites in the internal dendrimer structure. Heating of the 6.5 and 7.5 G-SBD at high pH causes decomposition of the dendrimers, whereas lower generation dendrimers show good thermal stability. The evaluation of the Cu(II) bonding parameters, α^2, α'^2, and β_1^2, indicates substantial covalency of the in-plane bonds, with the covalent character increasing respectively for the species corresponding to signal C, signal A, and signal B.

Introduction

Starburst dendrimers (SBDs) are a well-characterized novel class of macromolecules whose salient structural peculiarity is their fractal symmetry in constitution and shape with respect to the center of the molecule.[1] The synthesis of SBDs starts with a central core to which radially branched layers, termed generations, are covalently attached. The grafting of amidoamine units to a central nitrogen core generates the PAMAM family of SBDs (Figure 1), which was the first to be synthesized and characterized.[1a] Termination of the branches with amine groups produces the so-called full generation, or $G = n.0$, dendrimers. On the other hand, PAMAM dendrimers with carboxylate groups at the external surface are termed half-generation, or $G = n.5$, dendrimers. The fractal nature of the SBD structures precludes long-range order. Therefore, their morphologies and shapes have not yet been defined by X-ray spectroscopic techniques. However, molecular simulations[2] of the PAMAM dendrimers have indicated that the early full generations ($G = 1$–2) are characterized by asymmetric disklike shapes, which correspond to open structures that can be readily penetrated by solvent, whereas later generations ($G \geq 3$) possess a nearly spherical shape, which corresponds to closed, densely packed surface structures.

Recently, Moreno-Bondi *et al.*[3] have used the electron-transfer quenching of photoexcited $Ru(bpy)_3^{2+}$ by methyl viologen to investigate the structural differences between earlier and later

* To whom correspondence should be addressed: M. Francesca Ottaviani, Department of Chemistry, University of Florence, Via G. Capponi, 9, 50121 Firenze, Italy; Fax +39-55-244102.

† University of Florence.

‡ Columbia University.

§ Present address: Lehrstuhl fur Umweltmesstechnik der Universitat Karlsruhe, Engler-Bunte Institut, Richard Willstatter Allee 5, D(W) 7500 Karlsruhe 1, Germany.

∥ Michigan Molecular Institute.

® Abstract published in *Advance ACS Abstracts*, January 1, 1994.

(1) (a) Tomalia, D. A.; Baker, H. Dewald, J.; Hall, M.; Kallos, G.; Martin, S.; Roeck, J.; Smith, P. *Polym. J. (Tokyo)* **1985**, *17*, 117. (b) *Macromolecules* **1986**, *19*, 2466. (c) Tomalia, D. A.; Berry, V.; Hall, M.; Hedstrand, D. M. *Macromolecules* **1987**, *20*, 1164. (d) Tomalia, D. A.; Hall, M.; Hedstrand, D. M. *J. Am. Chem. Soc.* **1987**, *109*, 1601. (e) Padias, A. B.; Hall, H. K.; Tomalia, D. A.; McConnell, J. R. *J. Org. Chem.* **1987**, *52*, 5305. (f) Wilson, L. R.; Tomalia, D. A. *Polym. Prepr. (Am. Chem. Soc., Div. Polym. Chem.)* **1989**, *30*, 115. (g) Padias, A. B.; Hall, H. K.; Tomalia, D. A. *Polym. Prepr. (Am. Chem. Soc., Div. Polym. Chem.)* **1989**, *30*, 119. (h) Meltzer, A. D.; Tirell, D. A.; Jones, A. A.; Inglefield, P. T.; Downing, D. M.; Tomalia, D. A. *Polym. Prepr. (Am. Chem. Soc., Div. Polym. Chem.)* **1989**, *30*, 121. (i) Tomalia, D. A.; Naylor, A. M.; Goddard, W. A., III. *Angew Chem., Int. Ed. Engl.* **1990**, *29*, 138. (j) Tomalia, D. A.; Dewald, J. R. U.S. Patent 4,507,466, 1985; U.S. Patent 4 558 120, 1985; U.S. Patent 4,568,737, 1986; U.S. Patent 4,587,329, 1986; U.S. Patent 4 631 337, 1986; U.S. Patent 4,694,064, 1986; U.S. Patent 4,857,599, 1989.

(2) Naylor, A. M.; Goddard, W. A., III; Kiefer, G. E.; Tomalia, D. A. *J. Am. Chem. Soc.* **1989**, *111*, 2341.

(3) Moreno-Bondi, M.; Orellana, G.; Turro, N. J.; Tomalia, D. A. *Macromolecules* **1990**, *23*, 910.

0002-7863/94/1516-0661$04.50/0

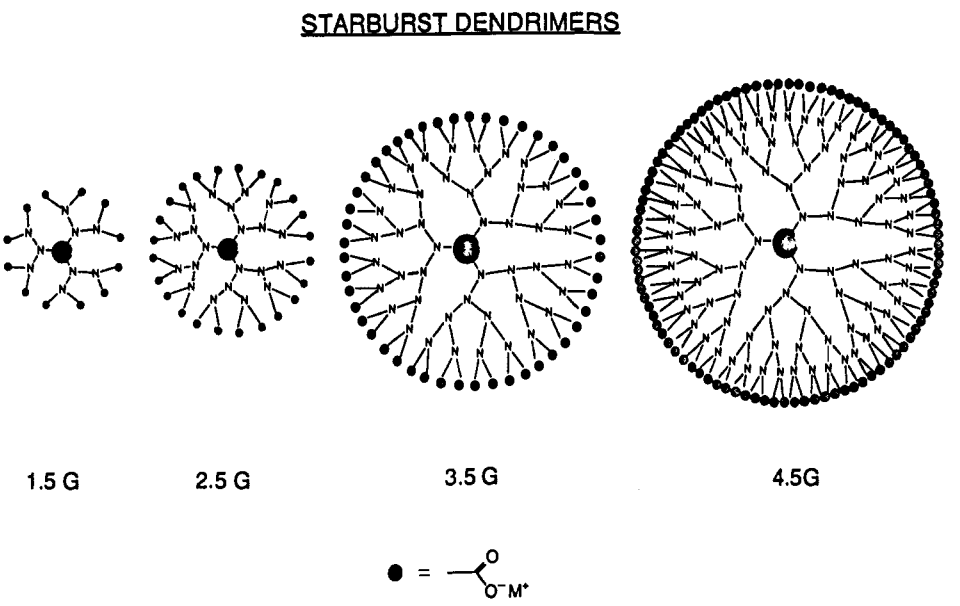

Figure 1. Two-dimensional projections of *n*.5 G-SBD, generations 1.5–4.5. Although schematic, the projections reveal the increasing density of potential N atoms as ligands in the increasing compactness of the external surface with increasing generation size.

generations of half-generation PAMAM dendrimers. The variations in the probe luminescence intensities and lifetimes support the change in morphology for the *n*.5 generations suggested by molecular simulations for the *n*.0 generations.

The *n*.5 generation dendrimers possessing anionic surfaces of sodium carboxylate groups (Figure 1) have been proposed as covalent mimics of anionic micelles.[1a,c,i] By using the photochemical intensity of the trisphenanthroline complex of ruthenium as a probe, Gopidas *et al.*[4] have obtained evidence by photophysical analysis on the similarities of the charged interfaces of PAMAM dendrimers and anionic micelles. A more complete characterization of the dendrimer surface would also require information on its binding capability, the extent of ionization in different experimental conditions, the ability to interact with molecules or ions, and the ability of molecules and ions to penetrate the internal core of the dendrimers. For instance, fluorescence spectroscopy was demonstrated by Caminati *et al.*[5] to be very advantageous in investigating the interactions of anionic and cationic surfactants with the PAMAM surface. From this point of view, the interaction of the negative surface with positively charged particles, such as metal ions, is expected to be very fruitful in characterizing the dendrimer surface and its interacting sites. The extent of ionization under various conditions may modify the binding capabilities and the mode of bonding involved in the complexation of surface groups with metal ions. On the other hand, starburst dendrimers and micelles clearly differ in the accessibility of the inner core to hydrophilic or hydrophobic particles. The close-packed, hydrophobic carbon chains which constitute the inner core of the micelles provide poor binding sites for hydrophilic components, which prefer to bind to the hydrophilic aqueous interface of the micelles. On the contrary, the inner core of SBDs is hydrophilic and potentially open to small hydrophilic molecules. An interesting question is whether small positively charged ions are able to enter the SBD structure and to coordinate various ligands at the internal surface. To a certain extent, the PAMAM internal structure resembles the structure of proteins and enzymes.[1a] Therefore, the mechanism of complex formation and the structure of the ion–internal site complexes at the PAMAM internal surface may have a biological relevance.

Electron paramagnetic resonance (EPR) has been a valuable tool for investigating complex equilibria involving Cu(II) ions in solutions at both high and low temperature (liquid and frozen samples).[6–8] For cupric complexes the dependence of the EPR parameters on coordinating atoms, geometry, and charge has been widely investigated.[8,9] Much work has been reported on the EPR spectra of copper complexes of biological interest.[7,10,11] The evaluation of magnetic parameters (main components of the **g** tensor for the Zeeman interaction and of the **A** tensor for the hyperfine interaction and the isotropic $\langle g \rangle$ and $\langle A \rangle$ values) at room and low temperatures provides information on the atomic type, the number of ligand groups, and the structure and dynamics of the complexes. Extended theories allow a detailed analysis of the EPR line shape,[12–14] which provides information on the mobility of the ions at the SBD surface and on the covalency of the coordinate bonding.[15]

The present report deals with the EPR study of Cu(II) complexes formed with the *n*.5 PAMAM dendrimers (from $G = 0.5$ to $G = 7.5$), henceforth called *n*.5 G-SBD, at different pH conditions, which should correspond to different degrees of protonation of the COO^- groups that form the external dendrimer layer. The availability of both surface COO^- and internal –N< and –NH–CO– binding sites makes possible the formation of different complexes, due to the distribution of Cu(II) at different sites, characterized by different ligands and/or different structural disposition of the ligands (modifications of the complex structure). Each of these complexes will give a contribution to the EPR line shape.

It is well established that copper usually forms dimeric complexes with carboxylate ligands such as carboxylic acids with short and long alkyl chains.[16,17] These complexes are EPR silent over a broad range of temperatures. We find that the EPR spectra

(4) Gopidas, K. R.; Leheny, A. R.; Caminati, G.; Turro, N. J.; Tomalia, D. A. *J. Am. Chem. Soc.* **1991**, *113*, 7335.
(5) Caminati, G.; Turro, N. J.; Tomalia, D. A. *J. Am. Chem. Soc.* **1990**, *112*, 8515.
(6) Hathaway, B. J.; Billing, D. E. *Coord. Chem. Rev.* **1970**, *4*, 143.
(7) Beinert, H. *Coord. Chem. Rev.* **1980**, *33*, 55.
(8) Addison, A. W. In *Copper Coordination Chemistry: Biochemical and Inorganic Perspectives*; Karlin, K. D., Zubieta, J., Eds.; Adenine Press: New York, 1983; p 109.
(9) Peisach, J.; Blumberg, W. E. *Arch. Biochem. Biophys.* **1974**, *165*, 691.
(10) Gould, D. C.; Mason, H. S. In *The Biochemistry of Copper*; Peisach, J., Aisen, P., Blumberg, W. E., Eds; Academic Press: New York, London, 1966; p 35.
(11) (a) Malmstrom, G.; Vanngard, T. *J. Mol. Biol.* **1960**, *2*, 118. (b) Aasa, R.; Petterson, R.; Vanngard, T. *Nature* **1961**, *190*, 258.
(12) McConnell, H. M. *J. Chem. Phys.* **1956**, *25*, 709.
(13) Kivelson, D. *J. Chem. Phys.* **1960**, *33*, 1094.
(14) (a) Freed, J. H.; Bruno, G. V.; Polnaszek, C. F. *J. Phys. Chem.* **1971**, *75*, 3385. (b) Polnaszek, C. F.; Bruno, G. V.; Freed, J. H. *J. Chem. Phys.* **1973**, *58*, 3185. (c) Goldman, S. A.; Bruno, G. V.; Polnaszek, C. F.; Freed, J. H. *J. Chem. Phys.* **1972**, *56*, 716.
(15) Kivelson, D.; Neiman, R. *J. Chem. Phys.* **1961**, *35*, 149.

of Cu–*n*.5 G-SBD are indicative of interactions with both nitrogen- and oxygen-centered ligands, but at low pH, complexation occurs at the dendrimer external surface and gives rise to monomeric copper–carboxylate complexes. The analysis of results from the Cu–*n*.5 G-SBD systems is based on many examples in the literature derived from monomeric copper complexes with carboxylate ligands, and in the presence of nitrogenous ligands,[18–23] or with a variety of biocompounds in which both nitrogen- and oxygen-centered ligands are present[7,11,24–30] at the surface of solid and/or polymeric structures.[31–34] Spectral analysis was conducted at various temperatures and pH to characterize both the mobility and the structural conditions of the complexes.

Experimental Section

The synthesis of SBDs has been described in previous papers.[1] The *n*.5 PAMAM family of dendrimers employed in this study (*n*.5 G-SBD; see Figure 1) falls in the range $G = 0.5$ to $G = 7.5$. Sodium carboxylate external groups were obtained by the hydrolysis of methyl ester-terminated generations with stoichiometric amounts of sodium hydroxide in methanol. Samples were thoroughly purified from water or methanol. However, dendrimers purified from methanol all gave solutions with very high pH (13–14), which, at any generation, displayed complexing behavior toward probes in the same manner as those at 0.5–1.5 generations, e.g., as observed with steady-state and time-resolved luminescence quenching experiments with Ru(II) complexes as probes (unpublished results). For the methanol-purified dendrimers, a decrease of pH by addition of HCl does not cause the SBD structure to be recovered. The EPR signal observed at high pH closely resembled that observed from the Cu(ethylenediamine)$_2$ complex.[23,35,36] These results suggest that purification from methanol causes a partial decomposition of the dendrimers, so that amino groups from the external layers can readily coordinate the copper ions. As a result of these complications with samples purified from methanol, we only describe results obtained from water-purified PAMAM dendrimers. These species were henceforth termed *n*.5 G-SBDs. Table 1 lists the molecular weights, the diameters obtained from SEC (size exclusion chromatography), the numbers of surface groups, and the calculated distances between surface groups for the different generation SBDs. The *n*.5 G-SBDs were used as aqueous solutions (1 mM in SBD macromolecules) for all experiments. After at least 24-h equilibration, portions of these solutions were added in stoichiometric amount to a 10 mM water solution of $Cu(NO_3)_2 \cdot xH_2O$ (Merck) to obtain a SBD macromolecule/Cu(II) ion molar ratio = 1. The samples were checked by EPR spectroscopy for both freshly prepared and aged at different "aging" times after preparation. The pH was changed (in the range 2–12) by adding controlled amounts of 0.1 M solutions of HCl and NaOH. The starting pH was set at 8.5, which corresponded to almost complete neutralization of the COOH groups for all the generations.

Table 1. Parameters Relevant to the Size and Surface Characteristics of Starburst Dendrimers

gen	MW	diameter[a]	surface gps[b]	sepn[c]
0.5	924	27.9	6	12.4
1.5	2173	36.2	12	12.8
2.5	4671	48.3	24	12.7
3.5	9668	66.1	48	12.6
4.5	19 661	87.9	96	11.5
5.5	39 648	103.9	192	10.3
6.5	79 621	126.8	384	9.8
7.5	159 568	147.3	768	7.7

[a] Diameters in angstroms determined by size exclusion chromatography (SEC) in water. [b] Number of surface groups. [c] Distance between surface groups in angstroms.

Steady-state and time-resolved luminescence quenching experiments (unpublished results) also reveal that Cu(II) quenches $Ru(phen)_3^{2+}$ much more efficiently when the latter is localized at the external surface of dendrimers, compared to solutions without dendrimers. This result is evidence that both the ruthenium complex and copper ions converge at or near the dendrimer external surface (i.e., at the interface between the dendrimer and the bulk aqueous phase). Furthermore, since the observed luminescence parameters do not change over time, the Cu–SBD systems in solution are stable over the duration of the experiments reported here. Water was distilled and further purified with a Millipore apparatus.

The EPR spectra were recorded by using a Bruker 200D spectrometer operating in the X band, interfaced with Stelar software to a PC-IBM computer for data acquisition and handling. The temperature was controlled with the aid of a Bruker ST 100/700 variable-temperature assembly. Magnetic parameters were measured by field calibration with the DPPH radical ($g = 2.0036$). A subtraction procedure (performed by means of the Stelar software) was used to obtain single-line signals from spectra which consisted of two or more overlapping signals. The addition of single-line signals also allowed the reproduction of the experimental pattern in case of superimposed contributions. With the aid of such a subtraction–addition method, the relative intensities of signals contributing to the overall line shape were also evaluated. The spectral line shape of frozen samples was also reproduced with the aid of the program CU23 (generously provided by Prof. Romanelli, Dept. of Chemistry, Firenze, Italy), based on the resolution of the spin Hamiltonian for copper complexes. The accuracy of the reported magnetic parameters is $A_{ii} = \pm 0.5 \times 10^{-4}$ cm^{-1} (about ±0.5 G), $g_{ii} = \pm 0.0005$.

The EPR spectra at low temperature never show the usual extra peak beyond the first hyperfine parallel component ($m_I = -3/2$) due to the ^{65}Cu(II) isotope ($I = 3/2$), whose natural abundance is 30.91%. This extra peak is probably not observable in the present case due to the broadness of the absorptions and to the overlapping of different absorptions.

The good reproducibility of results for the same experimental conditions provides support for the reliability of the results themselves and the structural stability of the Cu(II)–SBD systems over the time scale of the experiment.

Results and Discussion

(1) EPR Spectra of Cu(II)–*n*.5 G-SBD Complexes at pH 8.5. Figure 2a,b shows the EPR spectra at 293 K (Figure 2a) and 113 K (Figure 2b) for 0.5, 2.5, 3.5, 4.5, and 6.5 G-SBD at pH 8.5. The room temperature spectra reported in Figure 2a were recorded no later than 2–3 h after preparation of the samples, with the exception of spectra from 3.5 G-SBD, which were recorded 1 day after preparation. At room temperature, "earlier" generation dendrimers (0.5–2.5 G-SBD) exhibit different EPR features with respect to those exhibited by "later" generation dendrimers (3.5–7.5 G-SBD). For the earlier generations a rather well-resolved four-line hyperfine structure is observed and is assigned to the coupling of the electron spin with the copper nuclear spin ($I = 3/2$). The magnetic isotropic parameters of this signal, termed signal a, are $\langle a \rangle \approx 68$ G and $\langle g \rangle \approx 2.130$ (see insert labeled signal a in Figure 2a). Two other spectral contributions are present

(16) Melnik, M. *Coord. Chem. Rev.* **1981**, *36*, 1; **1982**, *42*, 259 and references therein.
(17) Bleaney, B.; Bowers, K. D. *Proc. R. Soc. London, A* **1952**, *214*, 451.
(18) Arena, G.; Coli, R.; Rizzarelli, E.; Sammartano, S.; Barbucci, R.; Campbell, M. J. M. *J. Chem. Soc. Dalton Trans* **1978**, 1090.
(19) Sharrock, P.; Melnik, M. *Can. J. Chem.* **1985**, *63*, 52.
(20) Szpakowska, M.; Uruska, I.; Stefanczyk, I. *Z. Anorg. Allg. Chem.* **1986**, *537*, 198.
(21) Greenway, F. T.; Pezesh, A.; Cordes, A. W.; Nobel, M. C.; Sorenson, J. R. *Inorg. Chim. Acta* **1984**, *93*, 67.
(22) Bhirud, R. G.; Srivastava, T. S. *Inorg. Chim. Acta* **1990**, *173*, 121.
(23) Valko, M.; Melnik, M.; Pelikan, P.; Valach, F.; Mazur, M. *Chem. Phys. Lett.* **1990**, *174*, 591.
(24) Sportelli, L.; Viti, V. *Stud. Biophys.* **1983**, *98*, 127.
(25) Kurzak, B.; Kurzak, K.; Jezierska, J. *Inorg. Chim. Acta* **1987**, *130*, 189.
(26) Harish, S. P.; Sobhanadri, J. *Inorg. Chim. Acta* **1985**, *108*, 147.
(27) Koide, M.; Tsuchida, E.; Kurimura, Y. *Makromol. Chem.* **1981**, *182*, 367.
(28) McBride, M. *Soil Sci. Soc. Am. J.* **1991**, *55*, 979.
(29) Gillard, R. D.; Lancashire, R. J.; O'Brien, P. *Transition Met. Chem.* **1980**, *5*, 340.
(30) Chapin-Swett, V.; Pitcher Dudek, E. *J. Phys. Chem.* **1968**, *72*, 1244.
(31) Nicula, A.; Stamires, D.; Turkevich, J. *J. Chem. Phys.* **1965**, *42*, 3684.
(32) (a) Vedrine, J. C.; Derouane, E. G.; Ben Taarit, Y. *J. Phys. Chem.* **1974**, *78*, 531. (b) Martini, G.; Bassetti, V.; Ottaviani, M. F. *J. Chim. Phys.* **1980**, *77*, 311. (c) Martini, G.; Bassetti, V. *J. Phys. Chem.* **1979**, *83*, 2511. (d) Clark, J.; McBride, M. B. *Clays Clay Miner.* **1984**, *32*, 300.
(33) (a) Peigneur, P.; Lunsford, J. H.; De Wilde, W.; Schoonheydt, R. A. *J. Phys. Chem.* **1987**, *91*, 1179. (b) Schoonheydt, R. A.; Peigneur, P.; Uytterhoeven, J. B. *J. Chem. Soc. Faraday Trans.* **1978**, *74*, 2550. (c) Martini, G.; Ottaviani, M. F. *Z. Naturforsh.* **1979**, *336*, 71.
(34) Rex, G. C.; Schlick, S. *J. Phys. Chem.* **1985**, *89*, 3598.
(35) Alei, M.; Lewis, B.; Denison, A. B.; Morgan, L. O. *J. Chem. Phys.* **1967**, *47*, 1062.
(36) Barbucci, R.; Campbell, M. J. M. *Inorg. Chim. Acta* **1976**, *16*, 113.

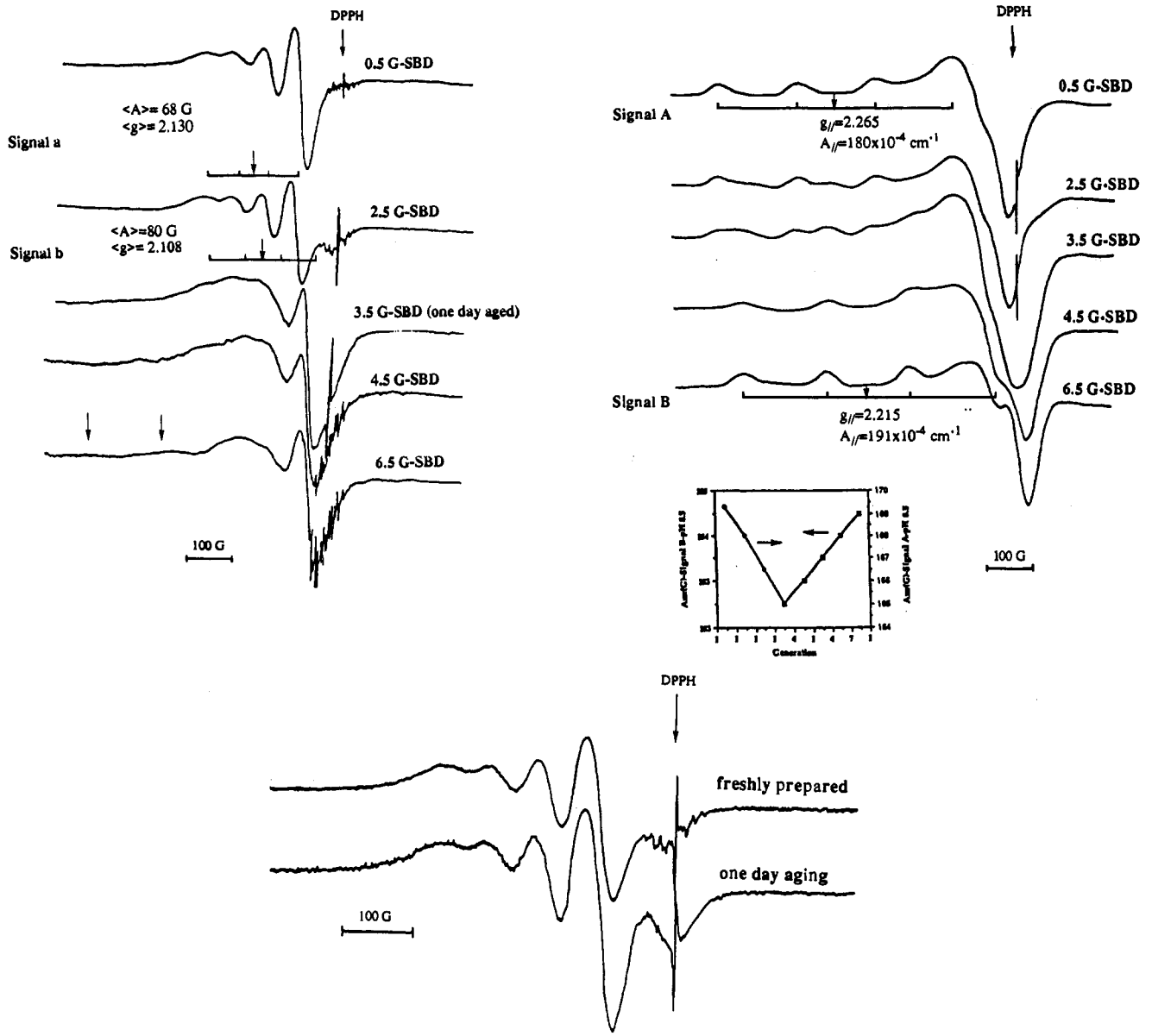

Figure 2. EPR spectra of Cu(II)–*n*.5 G-SBD, generations 0.5, 2.5, 3.5, 4.5, and 6.5 G at pH 8.5: (a, top left) 293 K; (b, top right) 113 K; in the inset the pattern for the variation of A_{zz} as a function of generation at pH 8.5 is reported; (c, bottom) 2.5 G-SBD freshly prepared and after 1 day of aging.

in the spectra in Figure 2a, superimposed on signal a. The first of these contributions is the four-line pattern, termed signal b in Figure 2a, whose highest field absorption (the fourth hyperfine line) clearly shows an increase in intensity with the increase of generation at the expense of signal a. The line shape of signal b is made evident by subtracting signal a from the spectra in which signals a and b are superimposed (see below). Signal b is characterized by a higher hyperfine isotropic coupling ($\langle a \rangle \approx$ 80 G) and a lower isotropic g value ($\langle g \rangle \approx 2.108$) compared to signal a (see the inset labeled signal b in Figure 2a).

The isotropic magnetic parameters listed in Figure 2a closely resemble those reported in the literature[28,37,38] for copper complexes in which both nitrogenous and oxygen ligands interact with the copper ion (to be discussed in detail, *vide infra*). A stronger interaction and/or a larger number of nitrogenous ligands is consistent with the variations of parameters on going from signal a to signal b.

There is also a third contribution to the room temperature spectra, which is detectable for the freshly prepared samples of any generation. This contribution appears (Figure 2a) as a multiline signal superimposed on the high-field absorption ($g \approx$ 2) and is typical of an organic nitrogen-centered radical. This signal is also present in the spectra of "pure" dendrimer solutions at pH 8.5, but its intensity is enhanced by Cu(II) addition. However, this radical signal disappeared approximately 1 day after preparation of the Cu(II)-containing samples, as is apparent from the spectrum of "aged" 3.5 solution shown in Figure 2a.

An expanded spectrum of a freshly prepared Cu(II)–3.5 G-SBD sample is displayed in Figure 3. This spectrum appears to arise from one unpaired electron localized on one of the nitrogens belonging to the amidoamine units constituting the internal structure of the dendrimers. Evidently these radicals form during the preparation procedure of the SBDs. We hypothesize that a redox reaction (probably Cu(II) → Cu(I) reduction) is responsible for the signal enhancement of this radical when copper ions are present. This assumption is supported by the finding that the disappearance of this signal over time corresponds to an increase in the intensity of signal b, as clearly shown by comparing the spectrum from a freshly prepared sample with that from an aged sample shown in Figure 2c for 2.5 G-SBD. The analysis of the radical signal, by means of spectral simulation (addition of Lorentzian lines), indicates that the unpaired electron couples with the nitrogen nucleus ($I = 1$), with hyperfine coupling constant $\langle a_N \rangle = 16.1$ G, and with the two inequivalent CH_2 groups linked

(37) Tikhomirova, N. N.; Zamaraev, K. I. *J. Struct. Chem.* **1963**, *4*, 200.
(38) Gampp, H. *Inorg. Chem.* **1984**, *23*, 1553.

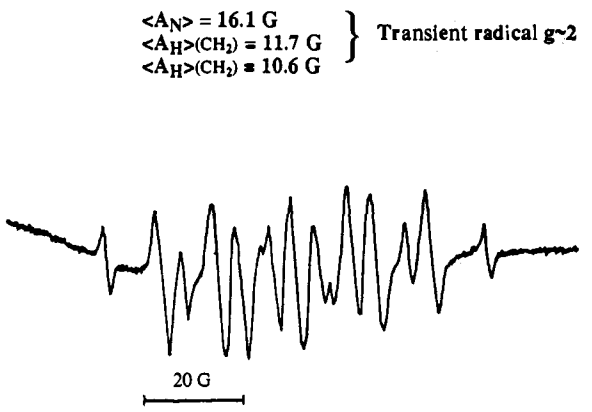

Figure 3. EPR spectra of the transient radical present for the freshly prepared Cu(II)–3.5 G-SBD systems.

to the nitrogen atom, with $\langle a_H \rangle$ = 11.7 and 10.6 G, respectively (a specific structure for this radical will be proposed below).

The 293 K spectra obtained from copper complexes with 3.5–7.5 G-SBDs are all characterized by a poorly resolved Cu(II) hyperfine pattern. One possibility for the observed broad line widths is a strong overlapping of the spectra of two or more species present in an equilibrium system.[10] However, in the present case, comparison with higher and lower temperature spectra (see below) excludes the possibility that the unresolved broad pattern may arise from broad overlapping lines of species in fast motion, i.e., dynamic equilibrium, conditions. On the contrary, the simultaneous presence of a well-resolved high-field absorption and broad low-field absorptions (indicated by arrows in Figure 2a) is typical of slow moving species. This is further supported by the results obtained from the analysis of spectra at different temperatures (see below). A slow motion condition means that the Cu(II) ions interacting at the *n*.5 (for $n \geq 3$) G-SBD surface are at least partially quenched in their rotational diffusion mobility. This may be due to the fact that the ligand groups belong to a macromolecule whose motion is slow in nature. However, the slowing of motion only appears for generations equal to or larger than 3.5, whereas for the lowest generations the spectra are characterized by faster mobility. This is supportive of the morphology information obtained from molecular simulation.[2] However, the decreased mobility observed for the higher generation dendrimers can be simply attributed to their larger molecular weight. Therefore, the EPR results allow earlier and later generations to be distinguished, on the basis of structural and dynamic parameters. By consideration of the SBD structure (Figure 1), it is inferred that Cu(II) ions are not confined at the SBD surface, but may enter the hydrophilic internal SBD structure and interact with the nitrogenous centers. Furthermore, it is also notable that Cu(II) distributes in two different environments whose relative contributions change in favor of the nitrogenous richer coordination shell as the generation size increases. The more open structure of the earlier generations and/or their lower molecular weight lead to faster mobility of the branches on which the copper ions are coordinated. In contrast, the compact, closed structure of the highest generations together with the increase in molecular weight is responsible for the reduction in mobility of the copper complexes. These results demonstrate copper ions to be good probes to analyze the SBD morphology.

In the low-temperature spectra (Figure 2b) two signals are clearly distinguishable, termed signals A and B, which correspond to the room temperature signals a and b, respectively. The relative intensities of the two signals also change (as do signals a and b at room temperature), showing an increase of signal B at the expense of signal A with an increase in generation. The magnetic parameters of both signals A and B slightly change from one generation to another. The variation of the **g** and **A** tensor components has been analyzed by means of spectral computation.

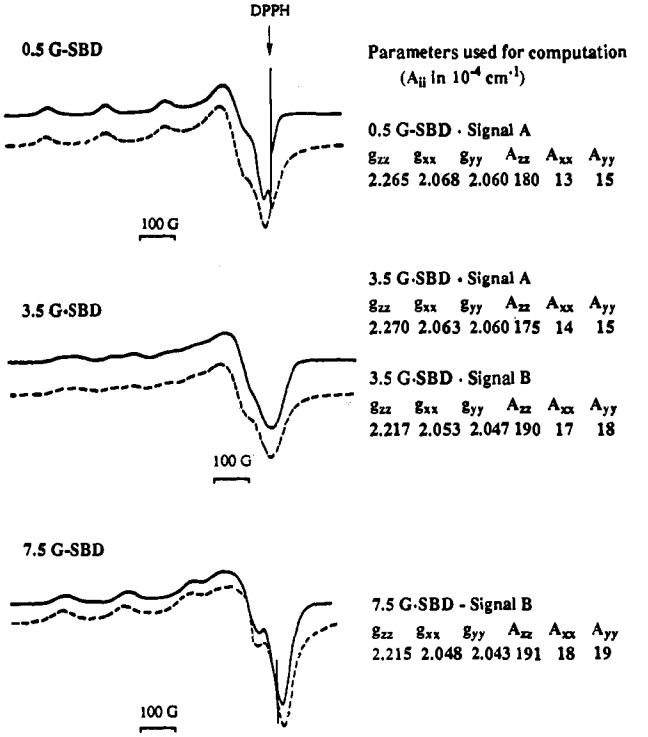

Figure 4. Experimental (solid lines) and computed (dashed lines) EPR spectra at 113 K of 0.5 G-SBD, 3.5 G-SBD, and 7.5 G-SBD, together with a list of the magnetic parameters used for the computation of the spectra.

Figure 4 shows the experimental and computed spectra of 0.5 G-SBD, 3.5 G-SBD, and 7.5 G-SBD together with the list of the magnetic parameters used for the computation. The trend is a small, but appreciable, decrease of $A_\parallel$ and an increase of $g_\parallel$ for signal A with an increase in generation, whereas the opposite holds for signal B. The insert in Figure 2b shows a graph for the variation of A_{zz} ($A_\parallel$) as a function of generation at pH 8.5 for signals A and B. The increase of $A_\parallel$ and the decrease of $g_\parallel$ have been shown to be a measure of the increase of the strength of the ligand bonding[15] (see the section on the evaluation of the bonding parameters). Therefore, with an increase in generation the complex responsible for signal B shows increasing stability, whereas the opposite holds for the complex associated with signal A.

We now seek to determine the specific structures responsible for the observed signals.

Several examples exist in the literature of magnetic parameters, evaluated for copper complexes, which are almost identical to those found for signals A and B (as examples, see refs 7, 11, and 20–30). From these literature parameters signal A is assigned a N_2O_2 coordination, i.e., two oxygen atoms from carboxylate groups and two nitrogens from the dendrimer interior. The magnetic parameters require three or four nitrogen ligands (N_3O or N_4 coordination) for signal B.

Figure 5 shows a possible structure for the localization of copper in the starburst dendrimer structure which would form the complexes responsible for signals A and B. Similar variation of magnetic parameters, as found from signal A to signal B, has been reported by several authors, due to an increase in the number of nitrogen ligands.[11,30,33a,b,35,36] In both cases the nitrogenous groups are positioned relatively far from copper, perhaps in a tetragonally distorted octahedral structure (for instance in the axial positions of the elongated octahedron), since no superhyperfine structure due to the coupling with the nitrogen nuclear spin is observed.[6,20,25] The increased relative intensity of signal B, compared to signal A, as a function of generation size is also supported on the basis of the starburst structure and the assigned structures of the complexes (Figures 1 and 5). The larger

Signal	Complex	G	Mobility (room T)	pH range
a,A	$Cu-N_2O_2$	0.5-2.5	fast	3.0-10.0
		3.5-7.5	slow	5.0-7.0
b,B	$Cu-N_3O$ or	0.5-2.5	fast	>8.0
	$Cu-N_4$	3.5-7.5	slow	>5.5
c,C	$Cu-O_4$	0.5-2.5	fast	<4.5
		3.5-7.5	fast	<6.0

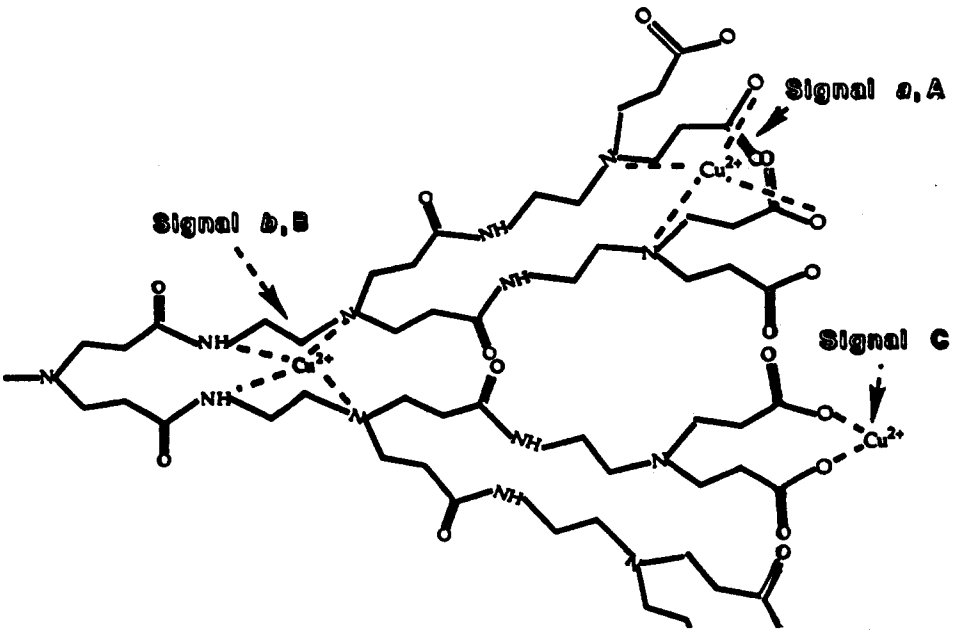

Figure 5. Structural section of *n*.5 G-SBD showing the suggested localization of Cu(II) to form the complexes responsible of signals a and A, signals b and B, and signal C.

dendrimers present a larger number of internal sites in which the compact structure may facilitate the interaction with more than two nitrogens, thus giving rise to signal B. It has been already pointed out that the open structure of the earlier generation SBDs allows a faster and easier exchange between the internal and the external regions.[3-5] As shown in Figure 5, we suggest that signal A originates from Cu^{2+} interacting with both surface carboxylate groups and nitrogens of the internal structure. This is of course facilitated in dendrimers possessing an open structure, e.g., 0.5–2.5 G-SBD. Thus, it is expected that signal A will be more dominant for the earlier generations.

Finally, the increase of signal b intensity at the expense of the signal of the radical indicates that a redox reaction occurs over time which corresponds to electron transfer from Cu(I) ions to the nitrogen containing the unpaired electron. It seems very probable that the nitrogen atoms involved in such electron transfer are directly coordinated to the Cu(I) ions. Therefore, on the basis of the structure of the radical, as inferred from the EPR signal features, the copper complex responsible for signal B should include, as ligand, a nitrogen bonded to two nonequivalent CH_2 groups.

(2) EPR Spectra of Cu(II)–*n*.5 G-SBD Complexes at Different pH. Figure 6 presents the EPR spectra recorded from 2.5 G-SBD at different pH, both at 293 (Figure 6a) and 113 K (Figure 6b). Parts a–c of Figure 7 present examples showing recovery of signals by spectral subtraction. At low pH, as shown in Figure 6a, the room temperature signal a changes its features, due to the superimposition with a new broad signal. The latter becomes distinguishable at low temperature and is superimposed on signal A. Spectral subtraction, as shown in Figure 7a, allows complete recovery of a new signal, termed signal C. The magnetic parameters of this additional signal are $A_\parallel = 150 \times 10^{-4}$ cm^{-1}, $g_\parallel = 2.361$, $g_\perp = 2.074$, as obtained from spectral computation. These values do not show any significant variation from one generation to another. The lowest pH spectra of the later generation SBDs contain only signal C, whereas signal A is detectable at pH $\geq$ 5 (results not shown). The parameters of signal C nicely match those already found by other authors for monomeric copper complexes with carboxylic acids[11,16,19,24,34] or for copper interacting with oxide surfaces, such as zeolites, silica gels, or aluminas.[31-33] Therefore, as shown in the assigned structure for signal C in Figure 5, each copper ion giving rise to signal C is coordinating two carboxylic groups (but interaction with an amide group cannot be excluded) at the external interface of the dendrimers. With increasing pH, signal C disappears as signal B emerges with increasing intensity at the expense of signal A. As shown in Figure 7b, the subtraction of the spectrum at pH 8.5 from the spectrum at pH 10 leads to almost complete

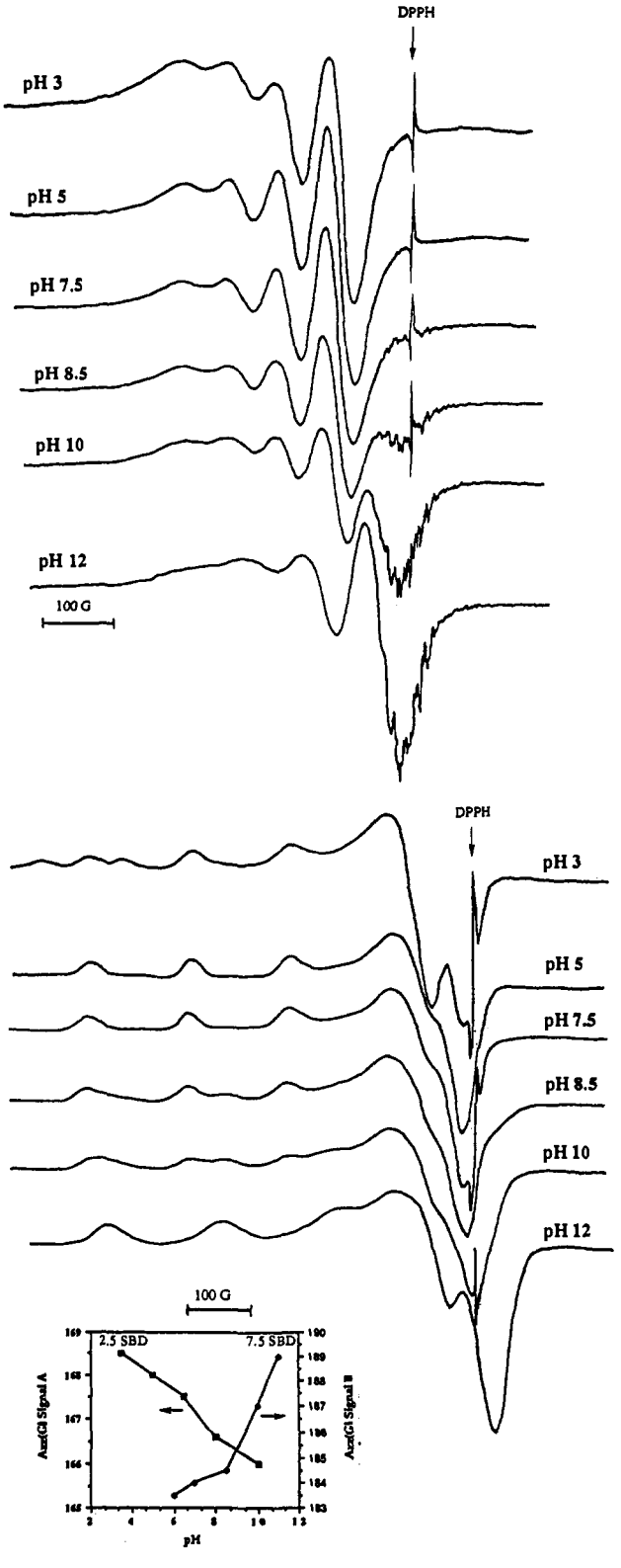

Figure 6. EPR spectra of Cu(II)–2.5 G-SBD at different pH: (a, top) 293 K; (b, bottom) 113 K. In the inset the graph shows the variation of A_{zz} as a function of pH for signal A (2.5 G-SBD) and signal B (7.5 G-SBD).

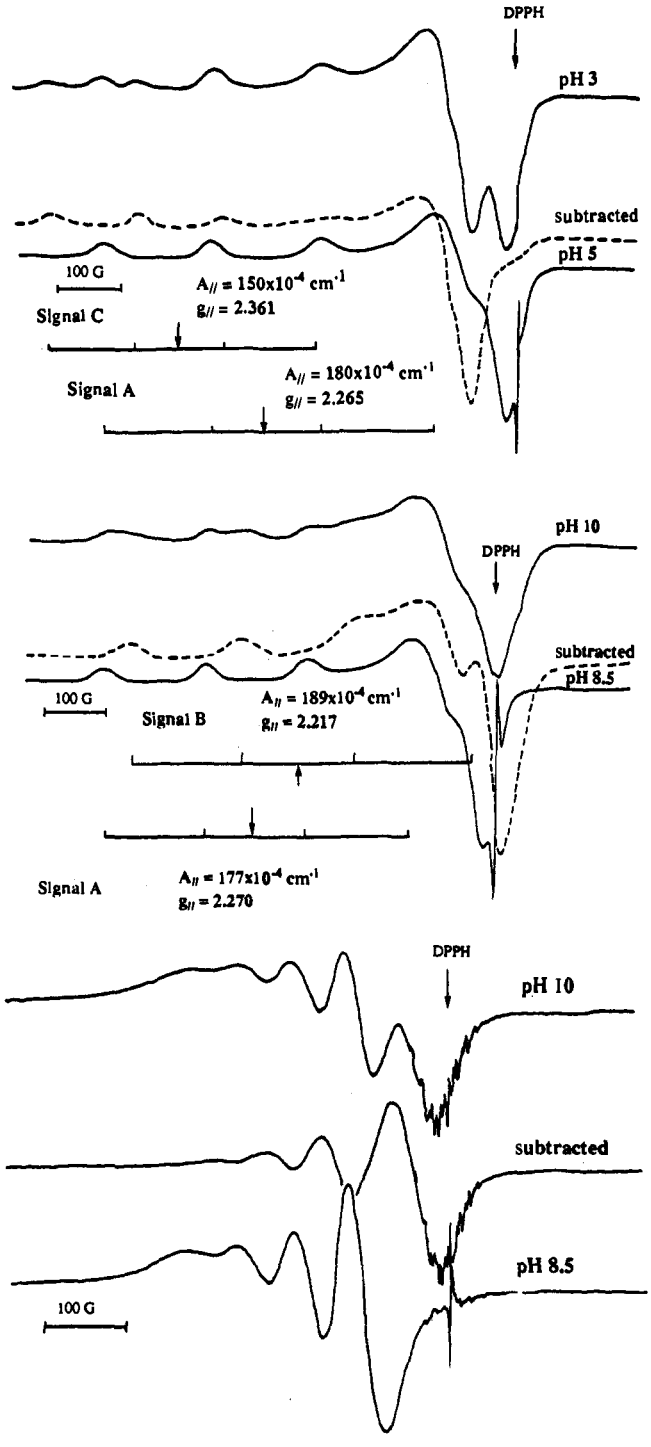

Figure 7. EPR spectra of Cu(II)–2.5 G-SBD at different pH: (examples of the subtraction procedure): (a, top) recovering of signal C from the 113 K EPR spectrum at pH 3 by subtraction of the spectrum at pH 5; (b, middle) recovery of signal B from the 113 K EPR spectrum at pH 10 by subtraction of the spectrum at pH 8.5; (c, bottom) recovery of signal b from the 293 K EPR spectrum at pH 10 by subtraction of the spectrum at pH 8.5.

recovery of signal B, which is the only contribution to the EPR line shape at pH 12. The spectra at room temperature show the same trend, and Figure 7c provides evidence for recovery of signal b by subtracting the room temperature spectrum at pH 8.5 from the one at pH 10 for 2.5 G-SBD. For the later generations, the low resolution of the room temperature spectra due to slow motion conditions prevents the determination of the relative intensity variation. However, it is noteworthy that the signal from the radical (see the previous section) appears connected to the appearance of signal b. Indeed, this radical works as a good indicator of the appearance of signal b, even when signal b intensity is so low that it is not detectable in the EPR spectra. This is further proof of a relationship between signal b and the signal of the radical and supports the assignment of the structure of signal B in Figure 5. Furthermore, as discussed in the previous section, the relative intensity of signal b increases when the radical signal disappears.

The magnetic parameters of signals A and B change slightly as a function of pH, as shown for $A_{zz} \equiv A_{||}$ in the insert in Figure

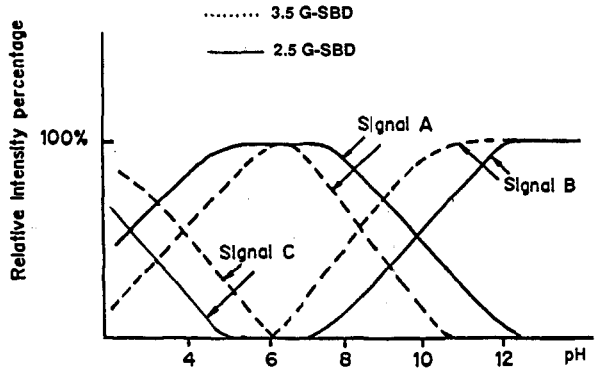

Figure 8. Variation of the relative intensity percentages of signals A, B, and C as a function of pH: solid lines, Cu(II)–2.5 G-SBD system; dashed lines, Cu(II)–3.5 G-SBD system.

6b. For instance $A_{\parallel}$ of signal B increases with an increase of pH, whereas the opposite holds for signal A. This again should reflect structural changes at the copper-binding sites, which modify the bonding parameters of the copper–ligand coordination bonds.[15] From the structural assignment in Figure 5, we can hypothesize a progressive removal of Cu(II) from the surface, which may enter more deeply into the SBD structure as the pH increases.

A combined analysis was performed by spectral subtraction and consequent double integration and by computation of the single components and consequent addition of the computed signals to fit the experimental spectra. Figure 4, already described in the previous section, shows an example for computing a spectrum consisting of two components, namely, the spectrum of 3.5 G-SBD at pH 8.5. On the other hand, Figure 7a–c shows examples of the subtraction procedure. The combined analysis, by means of computation and subtraction procedures, allows the evaluation of the relative intensities of the three signals, A, B, and C, at different pH, and for the various *n*.5 G-SBDs.

Figure 8 reports the relative intensity variation of signals A, B, and C as a function of pH for 2.5 G-SBD and 3.5 G-SBD. The relative intensities (uncertainty ±2%), obtained after subtraction and integration of the signal of each component, were measured at each pH unit in the range pH 2–13. In correspondence with the changes of slope, the subtraction–integration procedure was also carried out at half pH unit. As discussed in the previous section, signal B intensity increases with increasing generation. These results as a function of pH also indicate that signal B starts contributing at lower pH values for higher generations. What is evident by analyzing the graph in Figure 8 is the strong reduction in the range of signal A for 3.5 G-SBD with respect to 2.5 G-SBD. This range further diminishes for the higher generations, whereas it increases for the lower generations; but a larger gap between the extents of the ranges is found from 2.5 to 3.5 G-SBD, which is further evidence for the structural variation from the open structure of the 2.5 G-SBD to the more closed structure for 3.5 G-SBD. Indeed, the more densely packed structure of the later generation dendrimers gives rise to both a larger interaction of copper ions with the carboxylate groups at the interface at low pH and a larger interaction with the nitrogen richer sites at high pH. On the contrary, the dendrimers at lower generations display copper complexing with both terminal carboxylic groups and nitrogenous ligands over a large range of pH.

Various examples have been reported in the literature for systems which possess pH dependent equilibria between Cu(II) complexes and various combinations of coordinating nitrogen and oxygen atoms. For instance, refs 25 and 28 report on the variation from 1:1 Cu(II)/ligand, at low pH, to 1:2 Cu(II)/ligand, at high pH, for complexes between Cu(II) and ligands containing both nitrogen and oxygen ligand centers. Of course, the 1:2 complexes are characterized by a larger number of nitrogens in the copper coordination shell, if compared with the 1:1 complexes. However, other interpretations have been invoked to account for the spectral variations as a function of pH. For instance, Gampp[38] suggests, for $CONH_2$ groups, deprotonation at high pH of the NH_2 moiety, which consequently interacts with Cu(II) by substituting N as a ligand for the O of the CO moiety. Gillard and co-workers,[29] on the contrary, propose deprotonation of the water molecules coordinated to copper; that is, formation of hydroxylic complexes. In the present case, the internal branches of the SBD molecules contain CONH moieties and, also, water molecules, both of which can coordinate the Cu(II) ions. It is very improbable that deprotonation of the amide group occurs at pH 6, that is, the pH at which signal B starts appearing for the later generations. It is also very unlikely that such deprotonation will show such a strong dependence on the dendrimer generation. Therefore, we propose that the morphology modifications of the dendrimers together with the increasing availability of the internal sites are responsible for the observed variations from signal C to signal A to signal B as a function of pH. These variations, therefore, reflect the structural nitrogenous ligand enrichment in the copper coordination (Figure 5). However, a limited deprotonation of NH cannot be excluded as partially responsible for the observed variation of magnetic parameters (increase of $A_{\parallel}$ and decrease of $g_{\parallel}$) at high pH and for the contemporaneous appearance and enhancement of the signal from the radical.

(3) **Temperature Variations.** Figure 9 shows the EPR experimental spectra obtained at different temperatures for 2.5 G-SBD at high pH (pH 10–12, Figure 9, parts a and b, respectively) and for 4.5 G-SBD at pH 8.5 (Figure 9c). The decrease of line width, ΔB, with an increase of temperature (Figure 9a,c) indicates that the main relaxation mechanism is the rotational modulation of the anisotropic components of g and A tensors.[39] This effect gives rise, at high temperatures (fast motion conditions), to a direct proportionality between the line width and the correlation time for motion, which, in turn, is proportional to the viscosity/temperature ratio, on the basis of the Debye–Einstein approximation: $\Delta B \propto \tau_c \propto \eta/T$. A spin-rotational mechanism,[40] for which $\Delta B \propto \tau_c^{-1} \propto T/\eta$, is therefore not effective in the present case.

The fast motion conditions are due to rapid tumbling of the species in solution, at rates $(2–4) \times 10^{10}\ s^{-1}$, which causes averaging of the anisotropies. These conditions were found for the earlier generation dendrimers at room temperature and for the later generation ones at high temperatures. In the later generation dendrimers the tumbling rate is sufficiently slow to prevent averaging of the anisotropies. Indeed, the 268 K spectrum of 2.5 G-SBD resembles closely the spectra obtained at 293 K for *n*.5 G-SBD with $n \geq 3$. This result demonstrates that the slow motion conditions are sensed by copper ions trapped in the dendrimer structure for later generations. On the other hand, the dendrimers at later generations only recover a good resolution of the four lines at rather high temperatures. For instance, as shown in Figure 9c, it is necessary to increase the temperature to 348 K for 4.5 G-SBD to get a resolution equivalent to that for 2.5 G-SBD at room temperature. Further, by comparing parts b and c, of Figure 9, an almost "rigid" mobility was reached at about 248 K for 2.5 G-SBD and at 268 K for 4.5 G-SBD.

The SBD samples also show hysteresis in the spectral modifications with temperature. The 268 K spectrum of 2.5 G-SBD recorded with an increase in temperature after cooling shows slower mobility with respect to the 268 K spectrum obtained with a decrease in temperature (Figure 9b). However, 1 h of equilibration at each temperature gives a complete equivalence of the two spectra recorded with an increase and a decrease in temperature. The subtraction–addition procedure is very useful in clarifying the behavior at high temperature of samples which

(39) Wilson, R.; Kivelson, D. *J. Chem. Phys.* **1966**, *44*, 154.
(40) Poupko, R.; Luz, Z. *J. Chem. Phys.* **1971**, *57*, 3311. Atkins, P. W.; Kivelson, D. *J. Chem. Phys.* **1966**, *44*, 169.

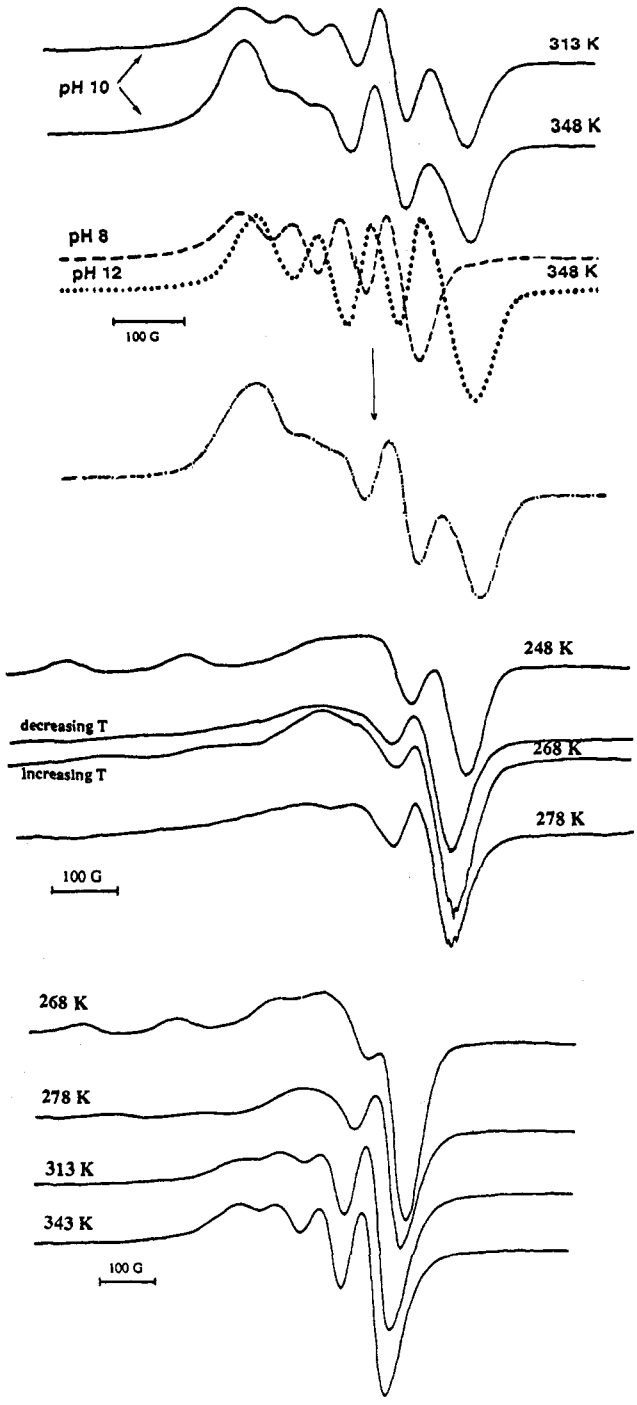

Figure 9. Examples of EPR spectra of Cu(II)–*n*.5 G-SBD at different temperatures: (a, top) 2.5 G-SBD at pH 10; the 348 K spectrum has been reproduced by summing the 348 K spectra at pH 8 and 12; (b, middle) 2.5 G-SBD at pH 12; the two 268 K spectra show the hysteresis in the patterns obtained by incr easing and decreasing the temperature; (c, bottom) 4.5 G-SBD at pH 8.5.

give rise to multicomponent spectra. For instance, the spectrum of 2.5 G-SBD at 348 K in Figure 9a seems broadened if compared to the spectrum at 313 K, whereas both signals a and b show line narrowing with an increase in temperature. The addition of signals a and b (at a ratio of about 1:1), as obtained at 348 K from 2.5 G-SBD at pH 8 and 12, respectively, nicely reproduces the experimental line shape of the 348 K spectrum at pH 10 (Figure 9a). The reason for the apparent but fictitious broadening is the decrease of the coupling constants with an increase in temperature. For instance, the isotropic coupling constant measured for 2.5 G-SBD at pH 6 decreases from 67.3 to 65.8 G as the temperature increases from 293 to 348 K, whereas a decrease of more than

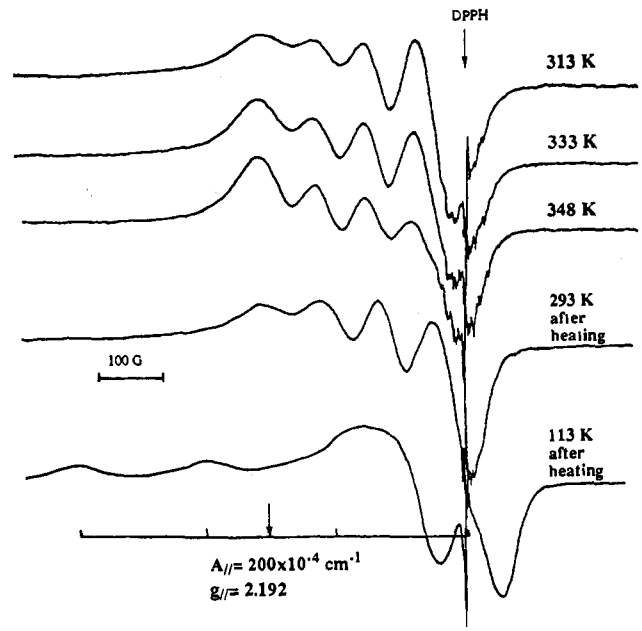

Figure 10. EPR spectra from Cu(II)–7.5 G-SBD at pH 10 as a function of temperature: at high temperature and, after heating, at 293 and 113 K.

2 G occurs for signal b at pH 12–13. The main effect is a partial overlapping of the two quartets (signals a and b), which gives, in some cases, a broad quartet instead of the characteristic five-line pattern found at room temperature.

An unexpected behavior is found for 6.5 and 7.5 G-SBD at high pH. Figure 10 shows the spectra recorded at high temperatures and, after heating, at room and low temperatures for 7.5 G-SBD at pH 10. The resolved four-line pattern recorded at high temperature is characterized by a higher coupling constant if compared to signal b. This pattern remains almost the same after subsequent cooling of the sample at room temperature. The high $A_{\parallel}$ (200×10^{-4} cm^{-1}) and the low $g_{\parallel}$ (2.192), evaluated from the low-temperature spectrum, are very close to those found for the samples purified from methanol (see Experimental Section) and are attributed to decomposition of the dendrimer external layers. It is noteworthy that the heating procedure did not give any effects of degradation for all the generations at any pH, only affecting 6.5 and 7.5 G-SBD at very high pH. Therefore, almost all the dendrimers in water solutions exhibit good thermal stability.

(4) Structure of the Cu(II)/SBD Complexes and Bonding Parameters. Table 2 lists the EPR magnetic parameters of the three signals (both room and low temperature) recorded for the *n*.5 G-SBD–Cu(II) system, mainly evaluated from spectral computation. We have chosen for the following analysis the sets of parameters characterized by the maximum and minimum $A_{\parallel}$ and $g_{\parallel}$ values found with the change of pH, which are listed in Table 2. These parameters are typical of Cu(II) ions in square-planar or tetragonally distorted octahedral coordination, with a $d_{x}2-_{y}2$ ground state. In order to discuss the nature of the copper–ligand bonding in terms of the magnetic parameters, the bonding parameters are calculated by a molecular orbital theory.[15,41] Since Cu(II) is a d^9 system, the "electron hole" notation is employed for evaluating the antibonding wave functions between the central atom 3d and the ligand 2s and 2p:

$$\varphi_{B_{1g}} = \alpha d_{x^2-y^2} - {}^1/_2\alpha'[-\sigma_x^{(1)} + \sigma_y^{(2)} + \sigma_x^{(3)} - \sigma_y^{(4)}]$$

$$\varphi_{B_{2g}} = \beta_1 d_{xy} - {}^1/_2(1-\beta_1^2)^{1/2}[p_y^{(1)} + p_x^{(2)} - p_y^{(3)} - p_x^{(4)}]$$

The $\varphi_{A_{1g}}$ wave function is omitted since it does not affect the

(41) Maki, A. H.; McGarvey, B. R. *J. Chem. Phys.* **1958**, *29*, 31–35.

Table 2. EPR Magnetic and Bonding Parameters of the Signals Recorded for the *n*.5 G-SBD–Cu(II) System[a]

signal	⟨g⟩	⟨A⟩[b]	$g_\parallel$	$A_\parallel$[c]	$g_\perp$	S	T(n)	E_{xy}[d]	α^2	α'^2
A, low pH	2.130	68.0	2.265	182.2	2.063	0.084[e]	0.277[e]	16 800[f]	0.84	0.24
A, high pH	2.132	66.0	2.270	174.5	2.063				0.82	0.26
B, low pH	2.108	78.0	2.220	189.0	2.052	0.093[g]	0.333[g]	18 300[h]	0.80	0.27
B, high pH	2.106	82.0	2.215	196.0	2.052				0.81	0.25
C	2.169[i]		2.361	150.0	2.073	0.076[g]	0.220[g]	14 200[j]	0.85	0.24

[a] For signals A and B (*a* and *b* at room temperature) for table reports the sets of parameters with the maximum and minimum $A_\parallel$ and $g_\parallel$ values found with the change of pH. [b] In gauss. [c] $\times 10^{-4}$ cm^{-1}. [d] In cm^{-1}. [e] Reference 33c. [f] Reference 43. [g] Reference 15. [h] Reference 44. [i] Evaluated from $\langle g \rangle = (2g + g_\parallel)/3$. [j] Reference 31.

magnetic parameters. The φ_{E_g} wave function is omitted, too, since it contains the parameter for out-of-plane covalent bonding, which is expected to be negligible.[15]

A measure of the covalency of the in-plane σ-bonding between a copper 3d orbital and the ligand orbitals is given by α^2, which can be evaluated in the first approximation by the equation

$$\alpha^2 = -(A_\parallel/P) + (g_\parallel - 2.0023) + {}^3/_7(g_\perp - 2.0023) + 0.04 \quad (1)$$

where $P = 0.036$ cm^{-1}, according to Abragam *et al.*[42] A measure of the covalency of the in-plane π-bonding is given by β_1^2, which can be evaluated from the equation

$$g_\parallel - 2.0023 = \frac{8\lambda_1\alpha\beta_1}{\Delta E_{xy}}[\alpha\beta_1 - \alpha'\beta_1 S - \alpha'(1-\beta_1^2)^{1/2}T(n)/2] \quad (2)$$

The values used for $T(n)$, the integral over the ligand functions, E_{xy}, the energy difference between E_{xy} and $E_{x^2-y^2}$, and S, the overlap integral, are taken from the literature[15,31,33c,43,44] and are listed in Table 2. The spin–orbit coupling constant for the free cupric ion is -828 cm^{-1}. The α'^2 is related to the interaction energy. The normalization of the in-plane σ-bonding orbital yields

$$\alpha^2 + \alpha'^2 - 2\alpha\alpha' S = 1 \quad (3)$$

By the use of eqs 1–3, the values of the bonding parameters, that is, α^2, β_1^2, and α'^2, were calculated. The obtained values are listed in Table 2.

As a measure of the covalency of the in-plane σ-bonding, $\alpha^2 = 1$ indicates complete ionic character, whereas $\alpha^2 = 0.5$ denotes 100% covalent bonding, with the assumption of negligibly small values of the overlap integral.[15] The β_1^2 parameter gives an indication of the covalency of the in-plane π-bonding. The smaller the β_1^2, the larger the covalency of the bonding. From this analysis, the in-plane bonds of the complexes correspondent to signals A, B, and C are largely covalent, with the covalent character increasing from signal C to signal A to signal B. The g values obtained from the EPR spectra indicate, as has been pointed out by Kivelson and Neiman[15] and by Faber and Rogers,[45] that covalent bonding reduces the magnitude of the g factors. Indeed, smaller g values and larger hyperfine coupling values are measured for signals b and B with respect to the others, which is consistent with the increased number of nitrogens in the coordination shell of Cu(II) (see Figure 5).

The variations of α^2 and β_1^2 in the different experimental conditions indicate structural modifications of the complexes with the experimental parameters. For instance, the data in Table 2 indicate that the covalency for signal B increases with an increase of pH, but only the in-plane π-bonding presents an increasing covalency. The same variations for the in-plane π-bonding occur for signal A at lower pH. A good agreement is found for the bonding parameters of signals A and B compared to those found for other copper complexes containing both nitrogenous and oxygen ligands, supporting the structural assignment of Figure 5.[15,30,46] On the other hand, copper complexes with exclusively oxygen ligands have been found to give bonding parameters close to those calculated for signal C, again supporting the structural assignment shown in Figure 5.

No appreciable differences in the bonding parameters are indeed observed among the dendrimers at different generations, and in any case, the differences in the bonding parameters at the various experimental conditions are very small. This finding is reliable proof for the homogeneity of the dendrimer structure over the different regions of the macromolecule, from one generation to another. This also demonstrates the stability of the structure of the complexes under the various experimental conditions.

Conclusions

EPR of copper complexes has proven to be a powerful tool to investigate the morphology of the starburst dendrimers and the structure and dynamics of Cu(II) complexes with the oxygen atoms of the surface carboxylate groups as well as with the internal nitrogen atoms. From a detailed EPR analysis of the aqueous solutions of half-generation PAMAM dendrimers containing Cu(II), three complexes could be identified. The structure of these complexes (Figure 5) was established from a comparison of the EPR parameters (**g** and **A** components) with similar parameters of **A** reported in the literature. The EPR line shape at room temperature indicates a variation in mobility of the Cu(II) complexes from 2.5 G-SBD to 3.5 G-SBD and is consistent with a change in the SBD morphology which results in a change in the motion of the Cu(II) complexes. Indeed at room temperature, for the early generation dendrimers, the complexes show fast mobility and suggest an openness of binding of the dendrimers. However for the later generations, even at room temperature, the complexes present slow motion, indicating a binding to a more compact dendrimer structure. Figure 5 summarizes the structural and dynamic information obtained from the analysis of the EPR spectra of the Cu(II)–*n*.5 G-SBD complexes. Complexation involving both the external carboxylic groups and internal nitrogen sites (signals a and A, which correspond to a Cu(II)–N_2O_2 coordination, Figure 5) is favored for dendrimers at lower generations in a large range of pH. The above findings are consistent with molecular simulation[2] for the *n*.0 G-SBD which leads to the expectation of a change in surface morphology occurring for the earlier generations near $n = 3$. A very good agreement is also found with the results obtained by means of photochemical and photophysical studies on the *n*.5 G-SBD.[3-5] Therefore, the EPR results support the classification into "earlier" generations, characterized by an open structure, and "later" generations, with a more spheroidal, close-packed structure. At low pH, copper ions interact only with the surface carboxylate groups (signal C, which corresponds to a Cu(II)–O_4 coordination, Figure 5), whereas at high pH, only the internal nitrogenous ligands are available for bonding (signals b and B, which correspond to a Cu(II)–N_4 coordination, Figure 5). This latter complex forms simultaneously with a transient radical with the

(42) Abragam, A.; Horowitz, J.; Pryce, M. H. L. *Proc. R. Soc. London, A* **1955**, *230*, 169.
(43) Fukuda, Y.; Sone, K. *Bull. Chem. Soc. Jpn.* **1971**, *45*, 465.
(44) Gordon, G.; Birdwhistell, R. K. *J. Am. Chem. Soc.* **1959**, *81*, 3567.
(45) Faber, R. J.; Rogers, M. T. *J. Am. Chem. Soc.* **1959**, *81*, 1849.
(46) Gersmann, H. R.; Swalen, J. D. *J. Chem. Phys.* **1962**, *36*, 3221.

electron spin centered on a nitrogen atom and coupling with two CH_2 groups. This allows the identification of at least one of the ligand groups as an amide in the complex, as shown in Figure 5.

The copper complexes formed into the close-packed structure undergo a remarkable decrease in their rotational mobility. The same decrease in mobility can be reached by the earlier generations at lower temperatures. Heating at high pH leads to decomposition of 6.5 and 7.5, G-SBD. A similar collapse of the dendrimer structure was shown by samples purified from methanol.

The homogeneity of the dendrimer structure is proved by the analysis of the bonding parameters of the complexes. The in-plane bonds possess a good covalent character, which increases with the increase of nitrogenous ligands in the complexes.

In summary, the computer-aided EPR analysis by using suitable paramagnetic probes can be profitably employed to investigate the structure of the starburst dendrimers and its modifications in several experimental conditions.

Acknowledgment. The authors at Columbia University thank the AFOSR and NSF for their generous support. D.A.T thanks the New Energy and Development Organization (NEDO) of the Ministry of International Trade and Industry of Japan (MITI) for the generous support and certain critical synthetic efforts. M.F.O. thanks the Italian Ministero Universita' e Ricerca Scientifica e Tecnologica (MURST), the Italian Consiglio Nazionale delle Ricerche (CNR), and NATO for their financial support.